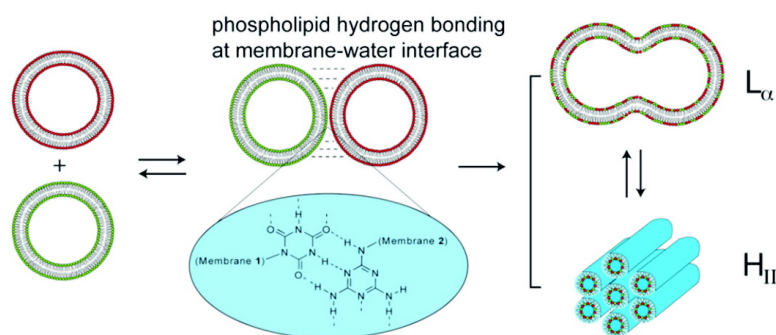


Intra- and Intermembrane Pairwise Molecular Recognition between Synthetic Hydrogen-Bonding Phospholipids

Mingming Ma, Angel Paredes, and Dennis Bong

J. Am. Chem. Soc., **2008**, 130 (44), 14456-14458 • DOI: 10.1021/ja806954u • Publication Date (Web): 14 October 2008

Downloaded from <http://pubs.acs.org> on February 8, 2009



More About This Article

Additional resources and features associated with this article are available within the HTML version:

- Supporting Information
- Access to high resolution figures
- Links to articles and content related to this article
- Copyright permission to reproduce figures and/or text from this article

[View the Full Text HTML](#)

Intra- and Intermembrane Pairwise Molecular Recognition between Synthetic Hydrogen-Bonding Phospholipids

Mingming Ma,[†] Angel Paredes,[‡] and Dennis Bong^{*†}

Department of Chemistry, The Ohio State University, 100 West 18th Avenue, Columbus, Ohio 43210, and
Department of Pathology and Laboratory Medicine, University of Texas Health Science Center,
Houston, Texas 77030

Received September 2, 2008; E-mail: bong@chem.osu.edu

Multivalency and preorganization are fundamental aspects of molecular recognition at the lipid membrane–water interface and can render weak monomeric binding interactions selective and robust; this concept is important throughout biology, biotechnology, and materials science.¹ We previously described how small molecule recognition between membranes is sufficient to selectively merge vesicular membranes;^{2,3} recent reports have indicated similar membrane chemistry directed by nucleic acid recognition.⁴ These systems all utilize hydrogen bond (H-bond) donor–acceptor pattern recognition between complex natural products or large biomolecules to guide membrane chemistry, which prompted our examination of yet simpler hydrogen bonding systems to study multivalent surface recognition in water. Intramembrane hydrogen bonding between native lipids has been well-documented and is thought to contribute to lipid bioactivity and membrane function.⁵ We hypothesized that avidity and preorganization effects at the lipid–water interface⁶ could overcome solvent competition and allow for selective hydrogen-bond recognition between small, unconstrained components. Lipid-mediated hydrogen-bonding interactions have been previously reported in bilayer,⁷ micellar,⁸ homovesicular,⁹ and weakly binding heterovesicular contexts;¹⁰ other heterovesicular recognition systems have been reported that are driven by metal-complexation^{11,12} and electrostatic¹³ interactions. We have found that electrostatically identical vesicular membranes composed of cyanuric acid and melamine functionalized phospholipids **1** and **2** undergo selective heterovesicular apposition, fusion, and adhesion in suspension and on solid support.

Mixtures of cyanuric acid (CA) and melamine (M) and derivatives are known to form hydrogen-bonded rosette, tape, and extended structures with 1:1 stoichiometry in organic solvents and solid state.¹⁴ While these interactions have not been experimentally demonstrated in aqueous solvent, it has been calculated that CA and M derivatives should interact strongly.¹⁵ We found that CA- and M-derivatized phospholipids **1** and **2** (Figure 1) could be dispersed in aqueous buffer to yield vesicles composed purely of **1** or **2**. This permitted careful examination of lipid assembly properties and dependence on membrane composition. Monosubstituted CA and M derivatives like **1** and **2** are known to form rosette or extended tape structures with six H-bonds per unit; this could also happen at the lipid–water interface. Interaction between lipids **1** and **2** was first probed in suspensions containing pyrene-functionalized lipid (Pyr-PC). The excimer–monomer (E/M) fluorescence intensity ratio of Pyr-PC is indicative of lipid mobility;¹⁶ vesicles composed of only **1**, **2**, or fluid-phase unsaturated lipid 1-palmitoyl-2-oleoyl-phosphatidyl-choline (POPC) all had similar E/M ratios with a linear temperature dependence, as expected for fluid, monophasic membranes. However, the 1:1 mixture of **1** and **2**

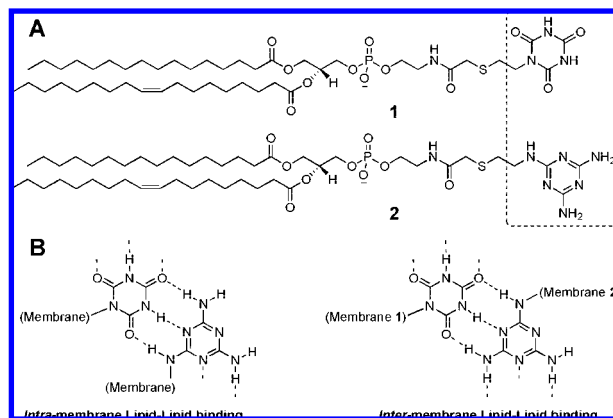


Figure 1. (A) Synthetic lipids **1** and **2**, headgroup functionalized with cyanuric acid and melamine (boxed), respectively. (B) Possible hydrogen-bonding patterns between lipids in intra- and intermembrane contexts. Dotted lines indicate possible hydrogen bonds.

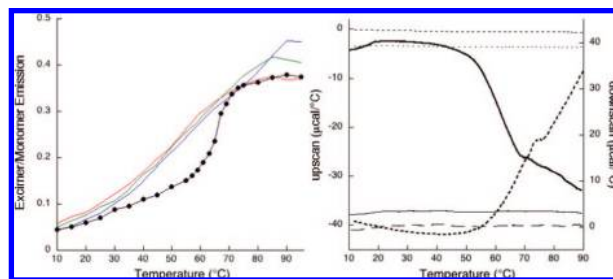


Figure 2. Intramembrane lipid recognition. (Left) Temperature dependence of pyrene PC excimer/monomer emission intensity in suspensions of **1** (red), **2** (blue), POPC (green), and a 1:1 mixture of **1** and **2** (black). (Right) DSC upscan (—) and downscan (---) traces of a suspension of a 1:1 mixture of **1** and **2**; **1** and **2** upscans (—, ···) and downscans (—, ---) are all flat traces.

behaved like a more rigid gel phase with a shallow phase transition at 22 °C and a sharper cooperative melting at 65 °C (Figure 2). Differential scanning calorimetry (DSC) revealed exothermic and endothermic peaks on the upscan at 20 and 75 °C, respectively; these transitions shifted¹⁷ on the downscan to 65 °C (exothermic) and 22 °C (endothermic). Together, the DSC and the pyrene data clearly indicate a temperature dependent phase transition that governs intramembrane lipid mobility, consistent with hydrogen bonding.

Surface plasmon resonance (SPR) was used to study intermembrane binding and reaction by flowing large unilamellar vesicles (LUVs) of **2** over surface bound **1** LUVs. The on-rate for adsorption was $\sim 40 \text{ M}^{-1} \text{ s}^{-1}$, though the off-rate at various solution concentrations was effectively zero, preventing calculation of an affinity constant. Desorption is often undetectable in SPR studies because of avidity and rebinding effects,¹⁸ but this could also be

[†] The Ohio State University.

[‡] University of Texas Health Science Center.

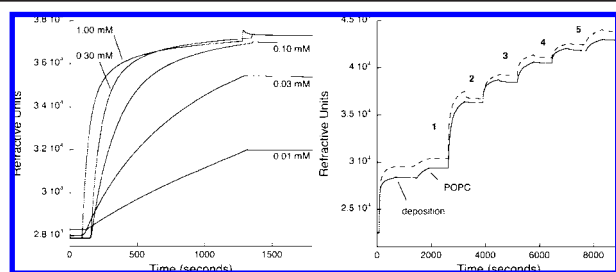


Figure 3. Intermembrane lipid recognition. (Left) Binding of surface anchored **1** with **2** at varying concentration as labeled. (Right) Refractive unit change upon deposition of **1** (—) and **2** (---) onto the bare SPR L1 chip followed by surface saturation with POPC and alternating treatment (numbered) with **2**, **1**, **2**, **1**, **2** (—) or **1**, **2**, **1**, **2**, **1** (---).

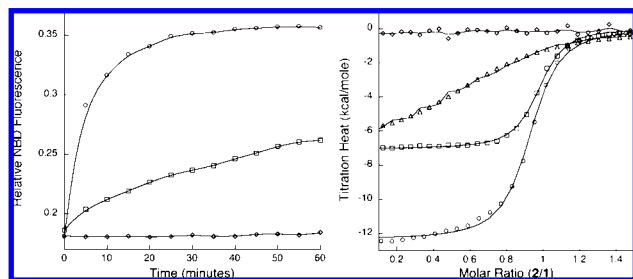


Figure 4. Intermembrane lipid recognition. (Left) Lipid mixing rates when LUVs containing 1.5% NBD-PE and 1.5% Rh-DHPE are reacted with unlabeled LUVs. The remainder of the reacting membrane compositions are **1** + **2** (○), 30% **1** in DPPC + 30% **2** in DPPC (□) and 50% **1** in POPC + 50% **2** in POPC (◇). (Right) ITC at 10 (○), 25 (□), 40 (△), and 50 °C (+) of injection of **1** LUVs into **2** LUVs. Markers indicate data points and solid lines are fits to 1:1 binding model.

due to irreversible fusion of suspension LUVs to the surface bound membrane (Figure 3). Indeed, treatment with **1** primed the surface for binding **2**, and vice versa, though alternating cycles of treatment resulted in decaying signal intensity (Figure 3). This ruled out “layer-by-layer” deposition and supports the fusion of tethered vesicles with suspended vesicles to produce a lipid mixed product that has diminished but residual affinity to both **1** and **2**. Importantly, the vesicles of **1** and **2** did not self-aggregate and deposit continuously on the SPR chip, nor did they react with neutral POPC membranes or POPG/POPC mixed membranes, but did react selectively and strongly with each other.

Selective intermembrane bonding between lipids **1** and **2** was also evident by dynamic light scattering (DLS); mixing **1** LUVs with LUVs of **2** resulted in a rapid and irreversible increase in particle size. Both phospholipid LUV suspensions had the same ζ -potential of -11 mV in PBS and thus bind each other despite electrostatic repulsion. Vesicle interaction was abrogated in low salt buffer, as a result of increased repulsion between the -33 mV ζ -potential surfaces under these conditions. Membrane apposition of **1** and **2** is accompanied by rapid lipid mixing (Figure 4) as judged by fluorophore dilution; similar to our previous findings, these events depend markedly on membrane composition. Vesicles prepared with POPC and **1** or **2** neither aggregated nor fused with each other at any mole ratio; however, replacement of POPC with dipalmitoyl phosphatidylcholine (DPPC) resulted in LUVs that aggregated (20% **1** and **2**) and LUVs that both aggregated and fused (30% **1** and **2**). These results likely derive from phase-separation of saturated DPPC from the unsaturated lipids **1** and **2** due to packing considerations; a single phase is expected with POPC. Phase-separation of DPPC from **1** and **2** would produce subdomains with a surface density of reactive lipids similar to a vesicle composed entirely of the interacting lipids, while a single domain

Table 1. Thermodynamics of Intermembrane Recognition^a

temp (°C)	ΔH (kcal/mol)	K_a (M^{-1})	ΔS (cal/K·mole)	ΔG (kcal/mol)
10	-12.4 ± 0.06	1.37×10^6	-15.5 ± 0.25	-7.96 ± 0.04
25	-7.04 ± 0.01	1.48×10^6	$+4.60 \pm 0.03$	-8.42 ± 0.002
40	-6.92 ± 0.07	6.73×10^4	0.0 ± 0.21	-6.92 ± 0.01
50				

^a Data fitting for K_a with a 1:1 binding model produced errors of 6.4%, 0.29%, and 1.47% for 10, 25, and 40 °C, respectively. No heat was detected at 50 °C.

mixed membrane would dilute surface ligand presentation and diminish reactivity.^{2,12}

Interestingly, the DLS and FRET data showed seemingly opposing temperature trends. The aggregation rate observed by DLS was much faster at 10 °C than at 25 °C, a result we attribute to enhanced hydrogen-bonding interactions at lower temperatures. However, the rate of lipid mixing was much faster at 25 than at 10 °C. This would suggest that although membrane apposition (driven by headgroup interaction) is more efficient at lower temperature, there is a thermal threshold for lipid mixing (lipid phase change) that exists between 10 and 25 °C.

Isothermal titration calorimetry (ITC) of the **1** + **2** vesicle reaction revealed a strongly exothermic 1:1 lipid interaction. Titration of freely soluble CA and M derivatives did not result in detectable heat flow (Supporting Information), indicating the strong effect of multivalent membrane presentation. Notably, the heat of interaction between **1** and **2** is context-dependent; lipid compositions that aggregate but do not mix have a significantly weaker negative enthalpy. The reaction becomes less exothermic with increasing temperature, with $\Delta H = -12$ kcal/mol at 10 °C, $\Delta H = -7$ kcal/mol at 25 °C, and nondetectable heat at 50 °C (Figure 4), consistent with DLS data that indicates loss of aggregation at 50 °C (Supporting Information). If six hydrogen bonds are formed on each CA and M, the upper limit set for enthalpic contribution from each hydrogen bond at the lipid–water interface is 1–2 kcal/mol, depending on temperature. The loss of vesicle recognition with higher temperature may be ascribed to a “melting” of the intermembrane lipid interactions, which occurs at a lower temperature than in the intramembrane context. Though the vesicle–vesicle interaction is a complex multivalent surface–surface adhesion coupled with lipid mixing and phase transition, the ITC binding curves fit remarkably well to a 1:1 binding model as a first approximation. Simple 1:1 fitting of the isotherms revealed that the ΔG_{rxn} at 10 °C is roughly the same as at 25 °C, -8 kcal/mol (Table 1). By this crude analysis, the reaction of **1** and **2** LUVs exhibits significant enthalpy–entropy compensation between these two temperatures, with enthalpy-driven reaction at 10 °C and both enthalpy and entropy change favorable at 25 °C. We speculated that the temperature-dependent change in ΔH and ΔS contributions signified a lipid phase-transition during membrane fusion from the lamellar phase to a more disordered morphology. Reaction stoichiometry was suggestive of complete fusion of the membranes at both temperatures, pointing toward the formation of a less-ordered nonlamellar phase at higher temperatures. Furthermore, ΔS at 40 °C is close to zero while the ΔH was similar to that found at 25 °C, indicating that the decreased driving force can be attributed completely to the less-favorable entropy change. This may be explained if the suspensions of **1** and **2** undergo a phase transition at a higher temperature (close to 40 °C), whereas the lipid mixture has a transition around 25 °C. Consistent with the formation of less reactive lipid phases of **1** and **2** at 40 °C, the calculated interaction stoichiometry at 40 °C was found to be 0.66 instead of 1:1.

Structural insight into the process of vesicle interaction and hypothesized changes in lipid phase morphology was sought through cryo-electron microscopy (cryo-EM), which indicated that LUVs

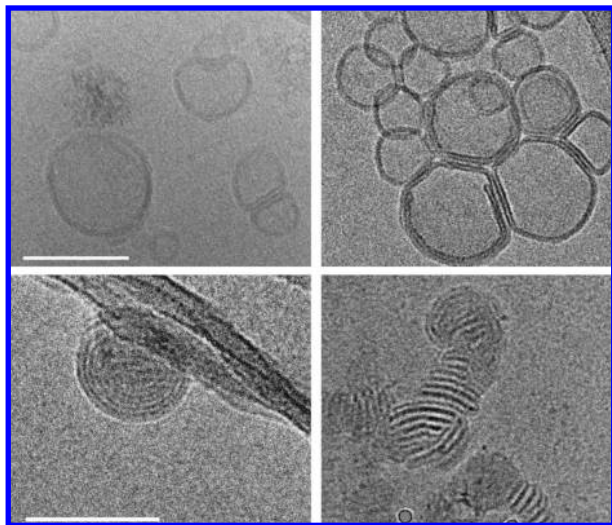


Figure 5. (Top left) Cryo-EM of **1** LUVs, (top right) **2** LUVs, (lower left) **1 + 2** premixed 1:1, (lower right) product of **1** LUVs reacted with **2** LUVs; round objects are gold beads. Scale bars (100 nm) in left panels apply to each row. All samples were prepared at room temperature.

of **1** and **2** appear morphologically similar and indeed are mostly unilamellar, dissociated vesicles that can be found as aggregates as well (Figure 5), consistent with DLS measurements. However, the structures derived from a 1:1 mixture of the two lipids, as well as the fusion product, are strikingly distinct from the pure vesicles and mechanistically suggestive. While the pure lipids produce vesicular structures that are mostly unilamellar, both the “premixed” lipids and the products of vesicle reaction appear to be in the hexagonal phase. Clear signatures of the hexagonal phase (presumably H_{II}) are observed as regular striations and lipidic structures consistent with interlamellar attachment sites (Figure 5).^{19,20} Some products of vesicle fusion are a combination of dense multilamellar vesicles that contain H_{II} phases within, while others appeared to be vesicles in the process of fusing (Supporting Information). Formation of a hexagonal phase is expected with strong lipid–lipid hydrogen bonding at the lipid–water interface as H-bonding between headgroups results in desolvation of the surface, which in turn permits high surface curvature and close membrane apposition through thinning of the repulsive hydration layer.⁵ Dehydration of the membrane and formation of the H_{II} phase should be entropically favorable,¹⁹ consistent with the ITC results. The lamellar (L_{α}) to H_{II} transition of the fused or mixed product of **1** and **2** is likely the low-temperature broad transition²¹ seen at 22 °C in the DSC and pyrene melt experiments. This could also explain the paradoxical observation of seemingly decreased aggregation and faster lipid mixing at 25 versus 10 °C. Fusion at 10 °C results in larger vesicles while fusion at 25 °C produces dense H_{II} phase particles that scatter light similarly to the starting vesicles (Figure 5). Thus, apposition has not decreased at higher temperature, but simply become less detectable by DLS. This is consistent with the reaction thermodynamics, which indicate equally facile interaction at both temperatures. Moreover, though not detected by DSC, it is possible that vesicles of **1** and **2** transition from the L_{α} to H_{II} phase around 40 °C, leading to the entropy-neutral reaction found by ITC. The structural and functional similarities between the **1 + 2** premixed suspensions and reacted **1 + 2** LUVs clearly demonstrate the notion that designed H-bond donor–acceptor interactions at the lipid–water interface can drive both intramembrane and intermembrane chemistry.

Though there are relatively few reports of designed, non-native aqueous phase hydrogen-bond recognition,^{6,22} this is commonly observed in native systems, most prominently in nucleic acid recogni-

tion. The system presented replaces the covalent sugar–phosphate scaffold of DNA with a noncovalently assembled phospholipid surface that also permits partial hydrophobic burial of the hydrogen-bonding groups upon heteromeric membrane apposition, similar to base-stacking and pairing. This finding underscores the presence of discriminating molecular recognition between two membrane surfaces which serves to optimize H-bond donor–acceptor interactions in both inter and intramembrane contexts and to minimize repulsive lone-pair interactions found in homomeric lipid hydrogen-bonding.

Finally, this study illustrates the general possibility of designing selective hydrogen-bonding adhesive interactions from simple starting materials at other polar–apolar interfaces;²³ this could have a numerous materials and biotechnological applications.^{1,24}

Acknowledgment. This work was supported in part by the University of Texas (A.P.), The Ohio State University, and an NSF-CAREER award to D.B. We thank the Structural Biology Imaging Center of University of Texas Health Science Center at Houston and the Ohio Bioproducts Innovation Center for support of the instrumentation used in this study.

Supporting Information Available: Synthetic and experimental procedures, lipid NMR and MS characterization, additional DLS, DSC, ITC, and cryo-EM data. This material is available free of charge via the Internet at <http://pubs.acs.org>.

References

- (1) Mammen, M.; Choi, S.-K.; Whitesides, G. M. *Angew. Chem., Int. Ed.* **1998**, *37*, 2754–2794.
- (2) Gong, Y.; Ma, M.; Luo, Y.; Bong, D. *J. Am. Chem. Soc.* **2008**, *130*, 6196–6205.
- (3) Gong, Y.; Luo, Y.; Bong, D. *J. Am. Chem. Soc.* **2006**, *128*, 14430–14431.
- (4) Chan, Y.-H. M.; van Lengerich, B.; Boxer, S. G. *Biointerphases* **2008**, *3*, 17–21. Stengel, G.; Zahn, R.; Hook, F. *J. Am. Chem. Soc.* **2007**, *129*, 9584–9585.
- (5) Boggs, J. M. *Biochim. Biophys. Acta* **1987**, *906*, 353–404.
- (6) Ariga, K.; Kunitake, T. *Acc. Chem. Res.* **1998**, *31*, 371–378.
- (7) Kawasaki, T.; Tokuyoshi, M.; Kimizuka, N.; Kunitake, T. *J. Am. Chem. Soc.* **2001**, *123*, 6792–6800. Kimizuka, N.; Kawasaki, T.; Hirata, K.; Kunitake, T. *J. Am. Chem. Soc.* **1998**, *120*, 4094–4104.
- (8) Nowick, J. S.; Cao, T.; Noronha, G. *J. Am. Chem. Soc.* **1994**, *116*, 3285–3289. Nowick, J. S.; Chen, J. S. *J. Am. Chem. Soc.* **1992**, *114*, 1107–1108.
- (9) Menger, F. M.; Zhang, H. *J. Am. Chem. Soc.* **2006**, *128*, 1414–1415.
- (10) Paleos, C. M.; Tsiourvas, D. *J. Mol. Recognition* **2006**, *19*, 60–67. Berti, D.; Baglioni, P.; Bonaccio, S.; Barsacchi-Bo, G.; Luisi, P. L. *J. Phys. Chem. B* **1998**, *102*, 303–308.
- (11) Lim, C. W.; Crespo-Biel, O.; Stuart, M. C. A.; Reinhoudt, D. N.; Huskens, H.; Ravoo, B. J. *Proc. Natl. Acad. Sci. U.S.A.* **2007**, *104*, 6986–6991. Waggoner, T. A.; Last, J. A.; Kotula, P. G.; Sasaki, D. Y. *J. Am. Chem. Soc.* **2001**, *123*, 496–497.
- (12) Mart, R. J.; Liem, K. P.; Wang, X.; Webb, S. J. *J. Am. Chem. Soc.* **2006**, *128*, 14462–14463.
- (13) Marchi-Artzner, V.; Gulik-Krzywicki, T.; Guedeau-Boudeville, M.-A.; Gosse, C.; Sanderson, J. M.; Dedieu, J.-C.; Lehn, J.-M. *ChemPhysChem* **2001**, *2*, 367–376.
- (14) Fyfe, M. C. T.; Stoddart, J. F. *Acc. Chem. Res.* **1997**, *30*, 393–401.
- (15) ten Cate, M. G. J.; Huskens, J.; Crego-Calama, M.; Reinhoudt, D. N. *Chem.–Eur. J.* **2004**, *10*, 3632–3639.
- (16) Galla, H. J.; Hartmann, W. *Chem. Phys. Lipids* **1980**, *27*, 199–219.
- (17) Sorrells, J. L.; Menger, F. M. *J. Am. Chem. Soc.* **2008**, *11*.
- (18) Nieba, L.; Kriebber, A.; Plockthun, A. *Anal. Biochem.* **1996**, *234*, 155–165.
- (19) Epanand, R. M. *Methods Mol. Biol.* **2007**, *400*, 15–26.
- (20) Frederik, P. M.; Burger, K. N. J.; Stuart, M. C. A.; Verkleij, A. J. *Biochim. Biophys. Acta* **1991**, *1062*, 133–141.
- (21) Wenk, M. R.; Seelig, J. *Biochim. Biophys. Acta* **1998**, *1372*, 227–36.
- (22) Oshovsky, G. V.; Reinhoudt, D. N.; Verboom, W. *Angew. Chem., Int. Ed.* **2007**, *46*, 2366–2393. Brunsvelde, L.; Vekemans, J. A.; Hirschberg, J. H.; Sijbesma, R. P.; Meijer, E. W. *Proc. Natl. Acad. Sci. U.S.A.* **2002**, *99*, 4977–4982. Brunsvelde, L.; Folmer, B. J. B.; Meijer, E. W.; Sijbesma, R. P. *Chem. Rev.* **2001**, *101*, 4071–4098. Hirschberg, J. H.; Brunsvelde, L.; Ramzi, A.; Vekemans, J. A.; Sijbesma, R. P.; Meijer, E. W. *Nature* **2000**, *407*, 167–170. Kato, Y.; Conn, M. M.; Rebeck, J., Jr. *Proc. Natl. Acad. Sci. U.S.A.* **1995**, *92*, 1208–1212. Ghadiri, M. R.; Granja, J. R.; Milligan, R. A.; McRee, D. E.; Khazanovich, N. *Nature* **1993**, *366*, 324–327.
- (23) Joh, N. H.; Min, A.; Faham, S.; Whitelegge, J. P.; Yang, D.; Woods, V. L.; Bowie, J. U. *Nature* **2008**, *453*, 1266–1270. Grigoryan, G.; DeGrado, W. F. *Nat. Chem. Biol.* **2008**, *4*, 393–394.
- (24) Madueno, R.; Raisanen, M. T.; Silién, C.; Buck, M. *Nature* **2008**, *454*, 618–621. Bong, D. T.; Clark, T. D.; Granja, J. R.; Ghadiri, M. R. *Angew. Chem., Int. Ed.* **2001**, *40*, 988–1011.

JA806954U